

Production of π^0 in the Coulomb field of nuclei by virtual photons from electron scattering

E. Hadjimichael

Physics Department, Fairfield University, Fairfield, Connecticut 06430

S. Fallieros

Physics Department, Brown University, Providence, Rhode Island 02912

(Received 16 November 1988)

We explore the cross section for π^0 production by virtual photons from electron scattering, interacting with the Coulomb field of heavy nuclei. The same process with real photons, generally known as the Primakoff effect, has been used in the past to investigate the π^0 lifetime. In the present work, virtual photons bring into focus the electromagnetic structure of the $\gamma\gamma\pi^0$ vertex.

I. INTRODUCTION

Whether one is committed to explaining nuclear phenomena in terms of an effective theory based on nucleons, isobars, and mesons, or one adopts a microscopic theory based on the quarks and gluons of quantum chromodynamics, one encounters the π meson as a crucial element of either theory. Consequently, its structure as it affects hadronic or electromagnetic interactions is a subject of intense interest. More specifically, the structure of hadronic and electromagnetic interaction vertices with pions, e.g., the πNN vertex and the $\gamma\pi\pi$ vertex, are of both practical and theoretical interest.

In the framework of the effective nuclear theory, one often uses phenomenological or semiphenomenological representations of vertex structure functions with parameters determined from precision fits of suitable data. The electromagnetic form factor of charged pions, for example, is often represented by

$$F_\pi(q^2) = \frac{1}{1 + \frac{q^2}{m_\rho^2}}, \quad (1.1)$$

where m_ρ is the ρ -meson mass and $q^2 = \mathbf{q}^2 - \omega^2$ is the four-momentum transferred to the vertex. This expression is based on the vector-meson dominance principle¹ (VMD) asserting that a photon couples to a π^\pm meson via an intermediate ρ meson. It seems to provide a reasonable first approximation to data.

There is no equivalent form factor characterizing the static structure of the neutral π^0 , since by charge conjugation the $\gamma\pi^0\pi^0$ vertex function vanishes. However, this particle can both be produced and decay via electromagnetic interactions involving virtual or real photons; these processes are then dependent on transition vertex structure functions or form factors, which have also been of theoretical and experimental interest for a long time.

The main decay mode of π^0 is

$$\pi^0 \rightarrow \gamma\gamma \quad (1.2)$$

while other electromagnetic decay modes with very small branching ratios are

$$\pi^0 \rightarrow \gamma^*\gamma \rightarrow e^+e^-\gamma \quad (1.3)$$

and

$$\begin{aligned} \pi^0 \rightarrow \gamma^*\gamma^* \rightarrow e^+e^- \\ \rightarrow e^+e^-e^+e^- \end{aligned} \quad (1.4)$$

The γ^* 's in these expressions denote virtual photons. The decay, Eq. (1.2), furnishes a direct way to measure the lifetime of π^0 .² Indirectly, this same quantity can also be measured by the Primakoff effect,³ i.e., the production of π^0 by the interaction of real photons with the Coulomb field of heavy nuclei. The cross section for this process is inversely proportional to the π^0 lifetime.

As a final point related to $\pi^0 \rightarrow \gamma\gamma$, one should recall that this decay mode has motivated the identification of the celebrated axial anomaly⁴ which modified in a crucial way the familiar partially conserved axial vector current (PCAC) relation for the axial current in the presence of electromagnetism.

The experimentally measured differential rate for the decay, Eq. (3), is expressed in terms of a vertex form factor

$$f \left[\frac{q_1^2}{m^2}, \frac{q_2^2}{m^2}, \frac{Q^2}{m^2} \right] = f(x, 0, 1), \quad (1.5)$$

where q_1 , q_2 , and Q are the four-momenta of the virtual photon, the real photon, and the pion, respectively, and m is the pion mass. This function is normalized by $f(0, 0, 1) = 1$, and for small x , it is written as

$$f(x, 0, 1) \equiv F_{\gamma\pi}(x) \approx 1 - ax. \quad (1.6)$$

Extracting a mean square radius from $F_{\gamma\pi}(x)$ in the usual manner, we may also write

$$F_{\gamma\pi}(q^2) = \frac{1}{1 + \langle r^2 \rangle \frac{q^2}{6}} \approx 1 - \langle r^2 \rangle \frac{q^2}{6}, \quad (1.7)$$

which leads to

$$a = \frac{\langle r^2 \rangle m^2}{6}, \quad (1.8)$$

and $\langle r^2 \rangle^{1/2}$ is an rms radius characterizing the $\gamma^* \gamma \pi^0$ interaction vertex.

Analysis of the $\pi^0 \rightarrow e^+ e^- \gamma$ data yields^{5,6}

$$a = \begin{cases} 0.05 \pm 0.03 & \text{(no radiative corrections)} \\ 0.1 \pm 0.03 & \text{(with radiative corrections)} \end{cases}. \quad (1.9)$$

Furthermore, assuming the validity of the VMD model for the transition vertex as well, and comparing with Eq. (1), we obtain the result

$$a = 0.03. \quad (1.10)$$

This value is in rather serious disagreement with that obtained from the $\pi^0 \rightarrow e^+ e^- \gamma$ data when radiative corrections are taken into account.

It is worth mentioning here, that an analogous process, namely, $\eta \rightarrow \gamma^* \gamma \rightarrow \mu^+ \mu^- \gamma$ (Ref. 7), has also been studied experimentally. The analysis of the data in terms of a form factor $F_{\gamma\eta}(q^2)$ gives a value for the form factor slope

$$a = 0.035 \pm 0.01, \quad (1.11)$$

in agreement with the VMD model prediction. In addition, the process $\gamma^* \gamma \rightarrow \eta'$ has also been measured in high-energy photon-photon collisions.⁸ Reasonable agreement with the predictions of a simple ρ^0 -pole model was reported.

Finally, the decay $\pi^0 \rightarrow e^+ e^-$ has been studied experimentally⁹ and its branching ratio was compared with theoretical predictions and found to disagree with these latter.

In the present work, we wish to study the π^0 production process by means of virtual photons of four-momentum q from electron scattering, interacting with the Coulomb field of heavy nuclei. This is nearly the reverse process of that in Eq. (3), since in reactions of this type, the four-momentum transferred to the nucleus through the electromagnetic field, is kept close to zero. However, in contrast to the decay, Eq. (3), where the virtual photon momentum is almost fixed and timelike, the process under consideration, shown in Fig. (1), is probed by a variable spacelike photon.

Our objective is to evaluate the cross section for this process and assess its experimental measureability and its sensitivity to the transition form factor $F_{\gamma\pi^0}(q^2)$ which is at the focus of our interest. We choose to denote thus this form factor, because one may view the production process as a transformation of a photon into a π^0 , probed by another virtual photon.

It is clear that the process under consideration is a natural extension of the Primakoff effect^{3,10,11} mentioned earlier, which has been studied and successfully exploited in the past for the purpose of determining the lifetime of π^0 and other pseudoscalar mesons. The current investigation extends the range of information to values of momentum transfer q different from zero and provides a kinematically more complete picture of the $\gamma\gamma\pi^0$ vertex.

We present the evaluation of the cross section of interest, and compare it to that for the Primakoff effect with real photons, in Sec. II of this article. Our results are displayed and discussed in Sec. III.

II. PRIMAKOFF EFFECT WITH VIRTUAL PHOTONS

We shall evaluate the coincidence cross section for the process shown in Fig. 1(a) with the kinematics of Fig. 1(b). Electrons of incident and outgoing momentum and energy (k_1, ϵ_1) and (k_2, ϵ_2) respectively, are scattered through angle θ_e , off the Coulomb field of a heavy nucleus (A, Z) . A π^0 meson of four-momentum $Q = (Q, \omega_\pi)$ and velocity $\beta_\pi = |Q|/\omega_\pi$ is produced electromagnetically via the process $\gamma^*(q) + \gamma(K) \rightarrow \pi^0(Q)$, where $\gamma^*(q)$ is a virtual photon of four-momentum q , from the scattered electron, and $\gamma(K)$ is a nearly real photon of four-momentum K from the Coulomb field of the nucleus. The latter is assumed to remain nearly stationary in its ground state, and hence its recoil energy K_0 is close to zero. It will be seen later that \mathbf{K} will have to be restricted to very small values as well.

We adopt a laboratory frame of reference with the z axis parallel to the three-momentum transfer q , and with the y axis in the $\mathbf{k}_1 \times \mathbf{k}_2$ direction. In this frame of reference, the pion angles are (θ_π, ϕ_π) . We treat the electrons relativistically, so that for $\epsilon_{1,2} \gg m_e, \epsilon_1 = |\mathbf{k}_1|, \epsilon_2 = |\mathbf{k}_2|$, and the four-momentum transfer square is $q^2 = 4\epsilon_1\epsilon_2 \sin^2 \theta_e / 2$.

For the $\gamma\gamma\pi^0$ vertex, we adopt the phenomenological interaction Hamiltonian density^{3,11}

$$H_I = \eta(\mathbf{B}_\gamma \cdot \mathbf{E}_N + \mathbf{E}_\gamma \cdot \mathbf{B}_N) \phi_\pi(x) \\ = \frac{i}{4} \eta \sum_{\mu\nu} \sum_{\sigma\tau} \epsilon_{\mu\nu\sigma\tau} F_{\mu\nu}^\gamma F_N^{\sigma\tau} \phi_\pi(x), \quad (2.1)$$

where the last expression is manifestly covariant. $(\mathbf{E}_\gamma, \mathbf{B}_\gamma)$ and $(\mathbf{E}_N, \mathbf{B}_N)$ are the electric and magnetic fields of the virtual photon and the nucleus, respectively, and $F_{\mu\nu}^\gamma$ and $F_N^{\sigma\tau}$ are the corresponding electromagnetic tensor operators, i.e., $F_{\mu\nu} = \partial_\mu A^\nu - \partial_\nu A^\mu$. We take the magnetic field of the nucleus to be $\mathbf{B}_N = 0$. $\phi_\pi(x)$ is the wave function of π^0 which we choose,

$$\phi_\pi(x) = \frac{1}{\sqrt{V}} \frac{1}{\sqrt{2\omega_\pi}} e^{-iQx} = \frac{1}{\sqrt{V}} \frac{1}{\sqrt{2\omega_\pi}} e^{-i(Q \cdot x - \omega_\pi t)}, \quad (2.2)$$

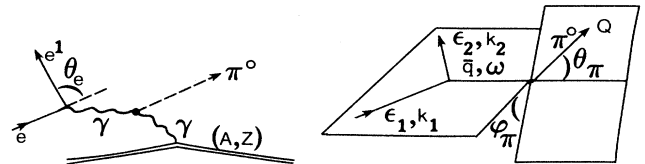


FIG. 1. (a) The Primakoff process with virtual photons from electron scattering; (b) kinematics for the process in (a).

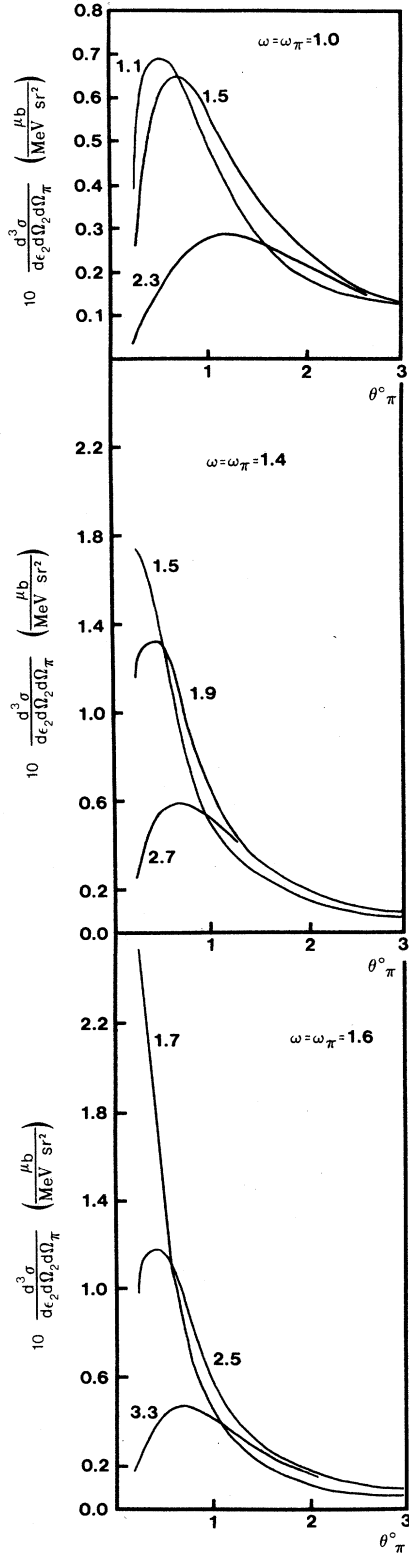


FIG. 2. The coincidence cross section for π^0 production from Pb, via the virtual-photon Primakoff effect, versus the pion angle θ_π , for several values of pion energy ω_π . Each curve is marked by the corresponding incident electron energy ϵ_1 . The electron scattering angle is $\theta_e = 5^\circ$ and the $\gamma^*\pi^0$ form factor slope, Eq. (1.6), is $a = 0.03$.

where V is the normalization volume. The coupling constant η in Eq. (2.1) is related to the π^0 lifetime by³ $\eta^2 = (4/\pi m^3)\tau^{-1}$.

In the present exploratory investigation, we disregard possible final-state interactions of the π^0 meson with the target nucleus, before π^0 decays, since the production process takes place in the Coulomb field of the nucleus, and not deep inside the nuclear volume.

The matrix element of the reaction amplitude S between initial and final states takes the form

$$\begin{aligned} \hat{S} &= \langle f; k_2 \lambda_2 | S | i; k_1 \lambda_1 \rangle \\ &= - \int \langle H_I(x) \rangle d^4x \\ &= - \frac{i}{4} \eta \sum_{\mu\nu\sigma\tau} \epsilon_{\mu\nu\sigma\tau} \int d^4x \hat{F}_{\mu\nu}^\gamma \hat{F}_N^{\sigma\tau} \phi_\pi(x), \end{aligned} \quad (2.3)$$

where

$$\hat{F}_{\mu\nu}^\gamma = \langle k_2 \lambda_2 | F_{\mu\nu}^\gamma | k_1 \lambda_1 \rangle, \quad \hat{F}_N^{\sigma\tau} = \langle f | F_N^{\sigma\tau} | i \rangle. \quad (2.4)$$

For the sake of simplicity, we avoid including in this expression at this time a nonlocal term representing the size of the interaction volume of the pion—a form factor in momentum space. This will be included later [see Eq. (2.11)].

The vector field \hat{A}_μ in the expression for $\hat{F}_{\mu\nu}^\gamma$ obeys the

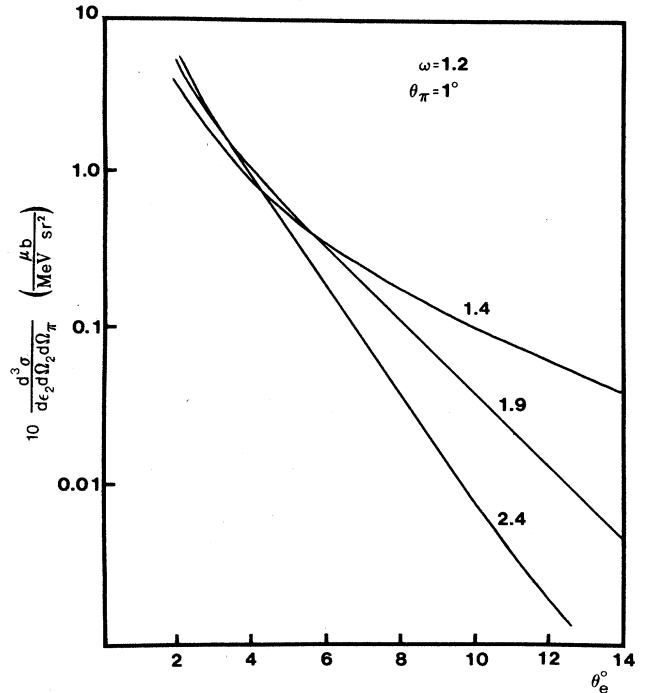


FIG. 3. The coincidence cross section versus the electron scattering angle θ_e , for two values of the pion energy ω_π . Each curve is marked by the corresponding incident electron energy. The pion angle is $\theta_\pi = 1^\circ$ and the $\gamma^*\pi^0$ form factor slope, Eq. (1.6), is $a = 0.03$.

well-known equation

$$\begin{aligned} \square \hat{A} &= -4\pi \hat{J}_\mu = -4\pi \langle k_2 \lambda_2 | J_\mu | k_1 \epsilon_1 \rangle \\ &= -4\pi i e \langle k_2 \lambda_2 | \bar{\psi}_e \gamma_\mu \psi_e | k_1 \epsilon_1 \rangle, \end{aligned} \quad (2.5)$$

where ψ_e is the quantized electron field. Evaluation of this equation yields

$$\hat{A}_\mu(x) = 4\pi \frac{ie}{V} \left(\frac{m_e^2}{\epsilon_1 \epsilon_2} \right)^{1/2} \frac{e^{iqx}}{q^2} j_\mu \quad (2.6)$$

(m_e is the electron mass), where

$$j_\mu = \bar{u}_{\lambda_2}(k_2) \gamma_\mu u_{\lambda_1}(k_1) = (\mathbf{j}, i\rho). \quad (2.7)$$

$u_{\lambda_i}(k_i)$ are the electron spinors and γ is the Dirac matrix. Introducing Eqs. (2.6) and (2.7) into the expression for $\hat{F}_{\mu\nu}^\gamma = \partial_\mu \hat{A}_\nu - \partial_\nu \hat{A}_\mu$ yields

$$\hat{F}_{\mu\nu}^\gamma = -\frac{4\pi}{V} e \left(\frac{m_e^2}{\epsilon_1 \epsilon_2} \right)^{1/2} \frac{e^{iqx}}{q^2} (q_\mu j_\nu - q_\nu j_\mu). \quad (2.8)$$

In addition, expressing $\hat{F}_N^{\sigma\tau}$ directly in terms of the electric field E_N (recall, $B_N=0$),

$$\hat{F}_N^{\sigma\tau} = \begin{pmatrix} 0 & 0 & 0 & -iE_1^N \\ 0 & 0 & 0 & -iE_2^N \\ 0 & 0 & 0 & -iE_3^N \\ iE_1^N & iE_2^N & iE_3^N & 0 \end{pmatrix}, \quad (2.9)$$

we find

$$\sum_{\mu\nu\sigma\tau} \epsilon_{\mu\nu\sigma\tau} \hat{F}_{\mu\nu}^\gamma \hat{F}_N^{\sigma\tau} = 16\pi \frac{ie}{V} \left(\frac{m_e^2}{\epsilon_1 \epsilon_2} \right)^{1/2} \frac{e^{iqx}}{q^2} \mathbf{E}_N \cdot (\mathbf{q} \times \mathbf{j}), \quad (2.10)$$

which gives for the matrix element

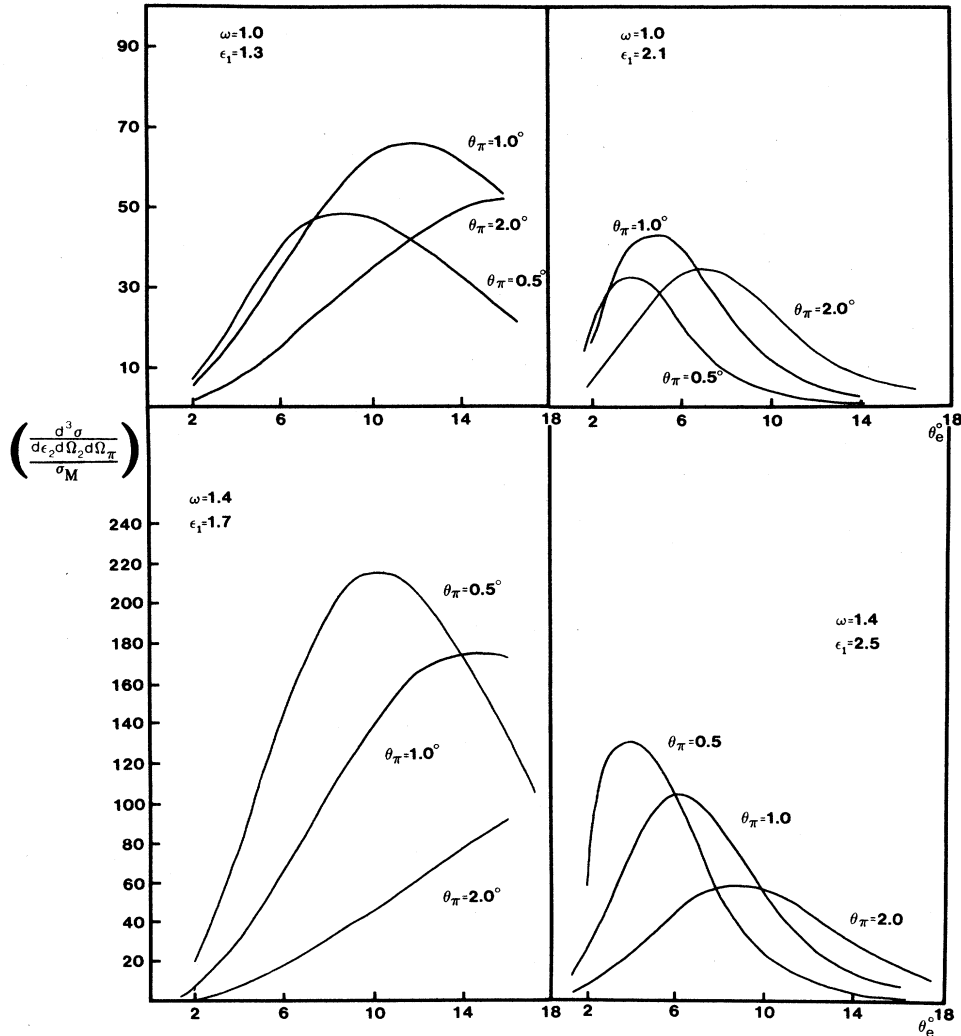


FIG. 4. Ratio R is the coincidence cross section to the Mott cross section which is expressed in $\text{MeV}^{-2}/\text{sr}$.

$$\hat{S} = 4\pi\eta \frac{e}{V^{3/2}} \left[\frac{m_e^2}{\epsilon_1\epsilon_2} \right]^{1/2} \times \frac{1}{q^2} \frac{F_{\gamma\pi}(q^2)}{\sqrt{2\omega_\pi}} (\mathbf{q} \times \mathbf{j}) \cdot \int d^4x e^{i\mathbf{K}\cdot\mathbf{x}} \mathbf{E}_N(\mathbf{x}). \quad (2.11)$$

Here we have written $K = q - Q = (\mathbf{q} - \mathbf{Q}, \omega - \omega_\pi)$ and have introduced the form factor $F_{\gamma\pi}(q^2)$ to represent the structure of the $\gamma^* \gamma \pi^0$ vertex.

The time part of the integral on the right side of Eq. (2.11) gives $2\pi\delta(\omega - \omega_\pi)$. To evaluate the remaining space part of this integral, we make use of the relationship of the electric field $E_N(\mathbf{x})$ with the nuclear charge

density $\rho_N(\mathbf{x})$ and obtain

$$\int e^{i\mathbf{K}\cdot\mathbf{x}} \mathbf{E}_N(\mathbf{x}) d\mathbf{x} = 4\pi i \frac{\mathbf{K}}{|\mathbf{K}|^2} \int e^{i\mathbf{K}\cdot\mathbf{x}} \rho_N(\mathbf{x}) d\mathbf{x}. \quad (2.12)$$

We define a nuclear charge form factor by

$$F_N(K^2) = \frac{1}{Ze} \int d\mathbf{x} e^{i\mathbf{K}\cdot\mathbf{x}} \rho_N(\mathbf{x}) \quad (2.13)$$

and arrive at the result

$$\hat{S} = (4\pi)^2 i Z e^2 \frac{\eta}{V^{3/2}} \frac{F_N(K^2) F_{\gamma\pi}(q^2)}{\sqrt{2\omega_\pi} |\mathbf{K}|^2} \times \left[\frac{m_e^2}{\epsilon_1\epsilon_2} \right]^{1/2} \frac{1}{q^2} \cdot 2\pi\delta(\omega - \omega_\pi) \mathbf{K} \cdot (\mathbf{q} \times \mathbf{j}). \quad (2.14)$$

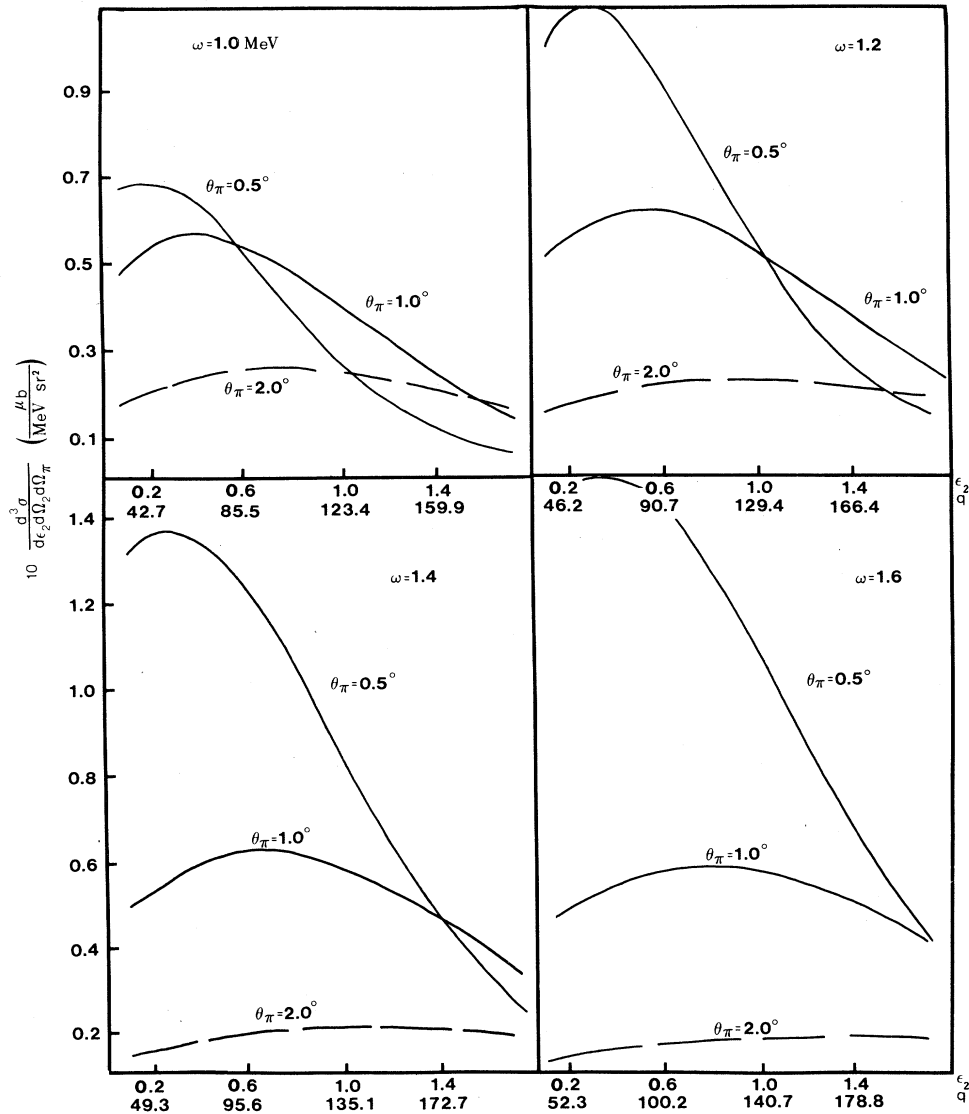


FIG. 5. The coincidence cross section versus outgoing electron energy ϵ_2 (in GeV) and four-momentum transfer q (in MeV/c), for several values of pion energy ω_π . Each curve is marked by the corresponding pion angle θ_π . The electron angle is $\theta_e = 5^\circ$ and the form factor slope, Eq. (1.6), is $a = 0.03$.

To obtain the cross section $d\sigma$, we require the incident electron flux given by $|\mathbf{k}_1|/V\epsilon_1$, and the final-state phase-space factor

$$V^2 \frac{d^3k_2}{(2\pi)^3} \frac{d^3Q}{(2\pi)^3}$$

so that

$$d\sigma = V^2 \frac{d^3k_2 d^3Q}{(2\pi)^6} \frac{1}{|\mathbf{k}_1|/V\epsilon_1} \frac{1}{2} \sum_{\lambda_1\lambda_2} \sum_i \sum_f |\hat{S}|^2. \quad (2.15)$$

Following straightforward manipulations, the coincidence cross-section differential in the scattered electron energy ϵ_2 and scattering angles Ω_e , and in the pion angles Ω_π , is

$$\frac{d^3\sigma}{d\epsilon_2 d\Omega_2 d\Omega_\pi} = \frac{Z^2 e^4 \eta^2}{\pi} \frac{1}{4\epsilon_1^2 \sin^4 \theta_e / 2} \frac{|F_N(K^2)|^2 |F_{\gamma\pi}(q^2)|^2}{|\mathbf{K}|^4} \frac{m_e^2}{\epsilon_1 \epsilon_2} \int d|Q| |Q|^2 \frac{\delta(\omega - \omega_\pi)}{\omega_\pi} \frac{1}{2} \sum_{\lambda_1\lambda_2} |\mathbf{j} \cdot (\mathbf{Q} \times \mathbf{q})|^2 \quad (2.16)$$

for a ground-state target nucleus with total spin $J=0$.

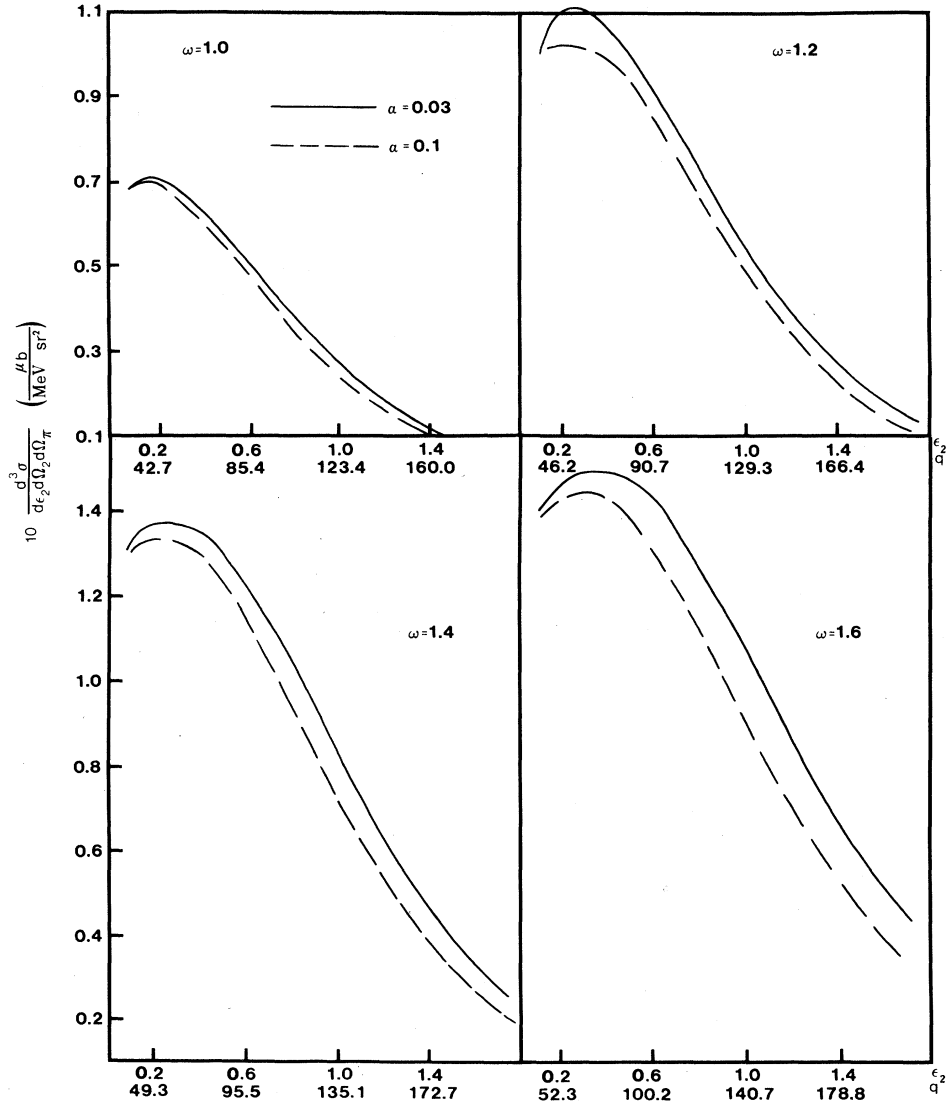


FIG. 6. The coincidence cross section versus the outgoing electron energy ϵ_2 (in GeV) and the four-momentum transfer q (in MeV/c), for four values of the pion energy ω_π , and at $\theta_e = 5^\circ$ and $\theta_\pi = 0.5^\circ$. The form factor slope, Eq. (1.6), is $a = 0.03$ for the solid line and $a = 0.1$ for the dashed line.

By employing trace theorems, we evaluate the sum over the electron helicities and find

$$\begin{aligned} \frac{1}{2} \sum_{\lambda_1 \lambda_2} |\mathbf{j} \cdot (\mathbf{Q} \times \mathbf{q})|^2 &= \frac{1}{m_e^2} \left[|(\mathbf{k}_1 \times \mathbf{k}_2) \cdot \mathbf{Q}|^2 + \epsilon_1 \epsilon_2 \sin^2 \frac{\theta_e}{2} |\mathbf{Q} \times \mathbf{q}|^2 \right] \\ &= \frac{\epsilon_1 \epsilon_2}{m_e^2} |\mathbf{Q}|^2 \cos^2 \frac{\theta_e}{2} \sin^2 \frac{\theta_e}{2} \sin^2 \theta_\pi \left[4\epsilon_1 \epsilon_2 \sin^2 \varphi_\pi + |\mathbf{q}|^2 / \cos^2 \frac{\theta_e}{2} \right] \end{aligned} \quad (2.17)$$

The last expression in Eq. (2.17) is based on the fact that \mathbf{q} is along the z axis and $\mathbf{k}_1 \times \mathbf{k}_2$ is in the y direction.

The first term in the bracket in Eq. (2.17) arises from the interaction of the magnetic field due to the electron orbital current, and the second term is due to the electron spin magnetic field. This result can also be clearly seen if one were to impose a Gordon decomposition on the electron current j , Eq. (2.7).

With Eq. (2.17), the integral in Eq. (2.16) is reduced to

$$\int d|\mathbf{Q}| \frac{|\mathbf{Q}|^4}{\omega_\pi} \delta(\omega - \omega_\pi) = \frac{|\mathbf{Q}|^4}{\omega_\pi} \beta_\pi^{-1} \Big|_{\omega=\omega_\pi} \quad (2.18)$$

and the coincidence cross section takes its final form

$$\begin{aligned} \frac{d^3 \sigma}{d\epsilon_2 d\Omega_2 d\Omega_\pi} &= \frac{Z^2 \eta^2}{\pi} \sigma_M \frac{Q^4}{\mathbf{K}^4} \frac{\beta_\pi^{-1}}{\omega_\pi} |F_N(K^2)|^2 |F_{\gamma\pi}(q^2)|^2 \\ &\quad \times \sin^2 \frac{\theta_e}{2} \sin^2 \theta_\pi \\ &\quad \otimes \left[4\epsilon_1 \epsilon_2 \sin^2 \varphi_\pi + |\mathbf{q}|^2 / \cos^2 \frac{\theta_e}{2} \right], \end{aligned} \quad (2.19)$$

where we have introduced the Mott cross section

$$\sigma_M = \frac{\alpha^2 \cos^2(\theta_e/2)}{4\epsilon_1^2 \sin^4(\theta_e/2)}. \quad (2.20)$$

It is of interest to compare this result with the cross section for the Primakoff effect with real polarized photons, which we have verified¹¹ to be

$$\frac{d^3 \sigma}{d\Omega_\pi} = 4\pi Z^2 \eta^2 \alpha \sin^2 \theta_\pi \sin^2 \varphi_\pi |F_N(K^2)|^2 \frac{Q^4}{\mathbf{K}^4} \beta_\pi^{-1}. \quad (2.21)$$

For unpolarized photons, we replace $\sin^2 \varphi_\pi$ by $\frac{1}{2}$ in Eq. (2.21).

While we see some similarities between Eq. (2.19) and Eq. (2.21), in particular in the angular dependence (θ_π, φ_π), there are also striking differences due to the extra electron-photon vertex in the case of π^0 electroproduction.

A detailed examination of Eq. (2.19) reveals that the cross section is optimized for $\theta_e \rightarrow 0$ and $\theta_\pi \rightarrow 0$, and for large values of energy transfer ω . Obviously, at $\omega^2 = \mathbf{q}^2$, i.e., at the photon point where $F_{\gamma\pi}(q^2) = 1$, we obtain no new information beyond that from the real-photon Primakoff effect.

III. RESULTS AND DISCUSSION

We shall evaluate the coincidence cross section for π^0 production by electron scattering, from the Coulomb

field of the Pb ($Z = 82$) nucleus.

It should be mentioned at this point that the process discussed here is experimentally distinguishable from the usual electroproduction which involves a hadronic meson-nucleon vertex. This is because the cross section for this latter peaks at higher values of, say, θ_π (Ref. 10) than the very forward values of this angle where our results will be shown to be optimized. It is therefore relatively easy to separate the two processes.

In the following we show results as a function of θ_π, θ_e , and energy transfer $\omega (= \omega_\pi)$. We shall examine the sensitivity of the cross section to the $\gamma^* \gamma \pi^0$ vertex form factor $F_{\gamma\pi}$. Recall that the coupling constant η is related to the π^0 lifetime τ . Taking $\tau = 0.869 \times 10^{-16}$ sec (Ref. 12) and the pion mass $m = 135.4$ MeV we find

$$\begin{aligned} \eta^2 &= \frac{4}{\pi m^3} \tau^{-1} = 4.4 \times 10^{16} \text{ fm}^3 / \text{sec} \\ &= 3.77 \times 10^{-12} \text{ MeV}^{-2}. \end{aligned} \quad (3.1)$$

Expressing σ_M in μb then the cross section in Eq. (2.19) will be expressed in $\mu\text{b}/\text{MeV} - \text{sr}^2$.

We use as input kinematics the variables $\epsilon_1, \omega (= \omega_\pi), \theta_e, \theta_\pi$, and φ_π . This latter angle is fixed at $\pi/2$. Furthermore, the results shown in Figs. 2–5 have been evaluated with the value $a = 0.03$ in the $\gamma^* \pi^0$ form factor, Eqs. (1.7) and (1.8), conforming to the VMD model. For the results in Fig. 6, $a = 0.1$ as obtained from fits of the $\pi^0 \rightarrow e^+ e^- \gamma$ data, has been used as well. These values of a were chosen because they define a reasonable range rather than in support of particular models.

In Fig. 2 we show the coincidence cross section as a function of pion angle θ_π , for six different values of the total pion energy ω_π , and for several incident electron energies. The strong forward peaking of the cross section is quite evident, and the optimization of the cross section for values of ω_π close to ϵ_1 anticipates the results in Fig. 3 showing it to peak at forward electron angles as well, which leads to nuclear recoil momentum $K \approx 0$. On this basis, we are justified to set the nuclear form factor $F_N(K^2) = 1$ in Eq. (2.19). This is obviously fortunate since it avoids the uncertainties associated with the determination of the nuclear form factor.

There is a certain advantage in examining our results in the form of the ratio R of the coincidence cross section to the Mott cross section in that this ratio highlights the structure effects of the π^0 production vertex. In Fig. 4 we plot R vs θ_e for different values of ω and ϵ_1 . As expected the angular distribution of R is different from that of the coincidence cross section itself which includes the familiar forward peaking of the Mott cross section.

In Fig. 5 we show the coincidence cross section versus ϵ_2 and the four-momentum transfer q at $\theta_e = 5^\circ$. We note that favorable kinematics is $\theta_\pi = 0.5^\circ$ to 1° , and moderate values of ϵ_2 , leading to small values of q^2 . This fact does not augur well for the sensitivity of this virtual-photon Primakoff effect to the $\gamma^*\pi^0$ form factor $F_{\gamma\pi}(q^2)$. Indeed, this sensitivity is displayed in Fig. 6 where we plot R vs ϵ_2 and q^2 , for several values of ω and for two values of the form factor slope, $a = 0.03$ and $a = 0.1$, as indicated in the beginning of this article. The corresponding values of the rms radius of the $\gamma^*\gamma\pi^0$ interaction volume, Eq. (1.6), are $\langle r^2 \rangle^{1/2} = 0.618$ and 1.13 fm. The impact of this large difference between the two values is mitigated by the small values of q^2 multiplying $\langle r^2 \rangle$ in the form factor,

Eq. (1.7), for which the cross section is optimal. Hence only a careful choice of kinematics will allow experimental discrimination between the right and wrong values of a or $\langle r^2 \rangle$. In general, values of incident electron energies and pion energies above 2 GeV are favored for probing the $\gamma^*\gamma\pi^0$ interaction vertex via the virtual-photon Primakoff effect. Such an experiment as this is recommended, because it will advance our understanding of photopion physics.

The work of one of us (S.F.) was supported by Department of Energy (DOE) Grant DE-FG02-87ER40334 and that of the other (E.H.) by National Science Foundation (NSF) Grant PHY-8711767.

- ¹M. Gourdin, Phys. Rep. **11**, 29 (1979); J. J. Sakurai, *Currents and Mesons* (University of Chicago Press, Chicago, 1969).
²G. von Dardel *et al.*, Phys. Lett. **4**, 51 (1963), and references therein.
³H. Primakoff, Phys. Rev. **81**, 899 (1957).
⁴S. Adler, Phys. Rev. **177**, 2426 (1969); J. Bell and R. Jackiw, Nuovo Cimento **60A**, 47 (1969); B. DeWit and J. Smith, *Field Theory in Particle Physics* (North-Holland, Amsterdam, 1986).
⁵K. O. Mikaelian and J. Smith, Phys. Rev. D **5**, 1763 (1972); G. E. Tupper, T. R. Grosse, and M. A. Samuel, *ibid.* **28**, 2905 (1983).
⁶J. Fischer *et al.*, Phys. Lett. **73B**, 359 (1978).

- ⁷R. I. Djhelyadin *et al.*, Phys. Lett. **94B**, 548 (1988).
⁸Ch. Berger *et al.* DESY Preprint No. 84-074, 1984; Phys. Lett. **149B**, 427 (1984).
⁹J. Fischer *et al.*, Phys. Lett. **73B**, 364 (1978).
¹⁰G. Belletini *et al.*, Nuovo Cimento **40**, 1139 (1965); **66A**, 243 (1970); V. I. Kryshkin *et al.*, Zh. Eksp. Teor. Fiz. **57**, 1917 (1969) [Soviet Phys.—JETP **30**, 1037 (1970)]; A. Browman *et al.*, Phys. Rev. Lett. **33**, 1400 (1974).
¹¹V. Glaser and R. A. Ferrell, Phys. Rev. **121**, 886 (1961); G. Morpurgo, Nuovo Cimento **21**, 569 (1974); G. Faldt, Nucl. Phys. **B43**, 591 (1972).
¹²Atherton *et al.*, Phys. Lett. **158B**, 81 (1985).